International Journal of Applied Mathematics in Control Engineering 3 (2020) 25-32

Contents lists available at YXpublications

International Journal of Applied Mathematics in Control Engineering

Journal homepage: http://www.ijamce.com

The Optimization of Global Secrecy Energy Efficiency in MIMO SWIPT Networks

Jinlong Wang*, Na Li, Datian Liu, Lin Zuo

School of Information and Electrical Engineering, Hebei University of Engineering, Handan, China.

ARTICLE INFO

Article history:
Received 12 January 2020
Accepted 15 March 2020
Available online 18 March 2020

Keywords:
Global secrecy energy efficiency
Multi input and multi-output(MIMO)
energy harvesting
Power splitting

ABSTRACT

The global secrecy energy efficiency is maximized in a multi-input and multi-output (MIMO) simultaneous wireless information and power transfer (SWIPT) networks, which is served by a central processing unit. By jointly configuring the power splitting factor, the precoding matrix, and the artificial auxiliary noise, and by considering the scheme that prevents the authorized devices' private information from eavesdropping, the optimization problem is formulated under the constraints of the required least harvested energy and the upper limit on the transmission power of the central processor. Due to the non-convexity of the fractional objective function in the formulated problem, a Two-level iterative algorithm based on Dinkelbach is proposed to solve it following the equivalent substitution, which converts the objective function to the subtractive form, and the approximation to the constraint. The simulation results validate the effectiveness of the proposed algorithm in improving global secrecy energy efficiency.

1. Introduction

With the gradual maturity of 5G technology, the Internet of Things (IoT) is expected to support wireless interconnection communication of billions of intelligent devices in the future. This will not only lead to a sharp increase in energy consumption [1,2,3], but also increase the risk of leakage of device privacy information [4]. Simultaneous wireless information and power transfer (SWIPT) meets the idea of green communications, and it's ability to recycle and reuse radio frequency energy has made this technology widely valued [5]. Ensuring the safe transmission of information at the IoT devices physical layer under energy saving conditions is a research hot spot in the field of green communication[6,7].

Secrecy energy efficiency (SEE) has become one of the key indicators to measure network performance due to its strong intuition and good sensitivity, and SEE is usually defined as the ratio of network secrecy rate and network energy consumption [8]. Currently, research on SWIPT technology based secrecy energy efficiency mainly focuses on Single Input Single Output (SISO) and Multiple Input Single Output (MISO) networks. In [9], the secrecy energy efficiency maximization of single-input single-output SWIPT network is studied under the constraints of user secrecy service quality and energy harvesting (EH), and the power allocation and power splitting (PS) factor are jointly optimized by Lagrange dual method and Dinkelbach algorithm. A new energy harvest receiver architecture is proposed in [10], in which the traditional EH receivers are divided into separate subunits. The PS factors in the subunits are optimized by dichotomous and successive convex approximation (SCA), and then the global optimum values of all variables are obtained using the Dinkelbach algorithm.

Since MIMO networks have different structural characteristics than the two aforementioned networks, and in MIMO networks, research efforts are focused on maximizing the secrecy rate of the networks [11,12]. In [11], the orthogonal projection method is used to optimize the precoding matrix of the EH receiver to completely suppress its interference with the information decoding (ID) receiver, and then the Taylor series expansion and the lagrangian dual method are used to optimizes the precoding matrix of ID receivers to maximize the network secrecy rate. The literature [12] uses semidefinite relaxation (SDR) and first-order Taylor series expansion to transform the original non-convex problem into a convex optimization problem, which by means of an iterative SCA algorithm and a singular value decomposition (SVD) method to obtain sub-optimal precoding matrix.

None of the above works consider the secrecy energy efficiency in SWIPT MIMO systems. In [13] , the Dinkelbach algorithm and the Taylor series expansion are introduced for maximizing secrecy energy efficiency in a three-node MIMO network , but all nodes are non-passive, which contradicts the energy-efficient character of green communication.

* Corresponding author.
E-mail addresses: jinlong_W1995@163.com (J. Wang)

Conventional secrecy energy efficiency is defined as the ratio between the achievable sum secrecy rate and the total required power. However, since the recovered energy of the IoT devices are from the energy supplying of the active device, therefore, the global secrecy energy efficiency (GSEE) indicator is proposed in this paper in MIMO SWIPT networks.

$$\text{GSEE[bits/ Hz/ J]} = \frac{\text{Worst secrecy rate[bps/ Hz]}}{\text{Total required transmit power[W]}}$$

This indicator calculates the energy efficiency based on the power consumption value of the active device and can be used as an objective function to achieve the highest secrecy rate. It also minimizes the power consumption of the active device, so it can evaluate the network performance more accurately. Since the channel state information of unauthorized EH devices is unknown, the central processing unit (CPU) in this paper models the channel based on the uncertainty of the channel state information. Then, the paper takes into account the authorized device information eavesdropping mechanism, and jointly configures the PS factor, precoding matrix and artificial auxiliary noise to maximize the global secrecy energy efficiency.

2. System Modeling

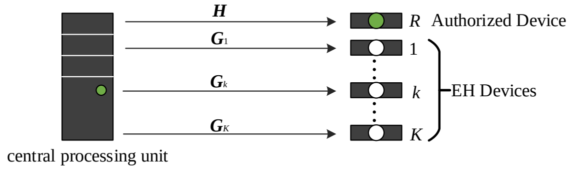

Fig. 1. The model of MIMO SWIPT Networks

This paper consider a downlink SWIPT IoT network, as shown in Fig.1. The system includes a CPU and (K+1) energy-constrained intelligent devices. Table 1 shows the comparison information of intelligent device in different time slots state. The CPU transmits information to only one device in a time slot, which is called an authorized device. The other K devices only harvest the energy of the radio frequency (RF) signal in the time slot, and these SWIPT energy devices are simply referred to as EH devices. In particular, in different time slots, authorized device and EH device can be converted to each other, as shown in Table 1. When the K EH devices are harvesting energy, they can choose to reject the charging and try to decode the received signal, thereby becoming a potential eavesdropper. The CPU and authorized device are equipped with N_T and N_R antennas respectively, while each EH device is equipped with N_E antennas. The authorized device R needs to feed back the channel state information to the CPU during the transmission. Therefore, it is assumed that the CSI of the authorized device R is perfect, and $\boldsymbol{H} \in \mathbb{C}^{N_T \times N_R}$ is used to represent the channel coefficient matrix of the authorized device. The CSI of K EH devices are uncertain, and the channel coefficient matrix of the k-th EH device can be modeled as [14]:

$$\boldsymbol{\Omega}_k = \{\boldsymbol{G}_k \,|\, \boldsymbol{G}_k = \widehat{\boldsymbol{G}}_k + \Delta \boldsymbol{G}_k, \|\Delta \boldsymbol{G}_k\|_F \le \delta_k\} \quad (1)$$
$$k \in \Pi = \{1, 2, 3, \ldots, K\}$$

where, $\widehat{\boldsymbol{G}}_k$ represents the estimated value of the channel coefficient matrix, $\Delta \boldsymbol{G}_k$ is channel estimation error, δ_k represents the radius of the channel uncertainty region, $\boldsymbol{G}_k \in \mathbb{C}^{N_T \times N_E}$.

In each time slot, the transmitted signal of the CPU includes the information sent to the authorized device and artificial noise, so the transmitted signal is expressed as Equation (2),

$$\boldsymbol{x} = \boldsymbol{W}\boldsymbol{s} + \boldsymbol{z}, \quad (2)$$

where, $\boldsymbol{W} \in \mathbb{C}^{N_T \times N_T}$ is precoding matrix, $\boldsymbol{s} \in \mathbb{C}^{N_T \times 1}$ is vector signals of unit norms, $\boldsymbol{z} \sim \mathcal{CN}(0, \boldsymbol{Z})$ represents artificial noise generated by the CPU. Therefore, the total transmit power of the transmitter is,

$$P_{\text{Total}}(\boldsymbol{W}, \boldsymbol{Z}) = \mu Tr(\boldsymbol{W}\boldsymbol{W}^H + \boldsymbol{Z}) + P_C, \quad (3)$$

where, $\mu \ge 1$ is the efficiency coefficient of the power amplifier, which depends on the information transmission process, P_C is the circuit power consumed by modules such as mixers, filters, and digital-to-analog converters.

The signals received by authorized device R and the k-th EH device are (4) and (5), respectively,

$$y_R = \boldsymbol{H}^H \boldsymbol{W}\boldsymbol{s} + \boldsymbol{H}^H \boldsymbol{z} + \boldsymbol{n}_R, \quad (4)$$

$$y_k = \boldsymbol{G}_k^H \boldsymbol{W}\boldsymbol{s} + \boldsymbol{G}_k^H \boldsymbol{z} + \boldsymbol{n}_k, \quad (5)$$

where, $\boldsymbol{n}_R \sim \mathcal{CN}(0, \sigma_R^2 \mathbf{I}_{N_R})$ and $\boldsymbol{n}_k \sim \mathcal{CN}(0, \sigma_k^2 \mathbf{I}_{N_E})$ are Gaussian white noise introduced by the authorized user and the k-th eavesdropping user antenna, respectively.

After the signal transmitted from the CPU is received by the authorized device, the authorized device divides the signal into two power streams $y_{R,I}$ and $y_{R,E}$ through a power splitter, where $y_{R,I}$ is used for information decoding and the other part $y_{R,E}$ is used for energy harvesting. The $y_{R,I}$ and $y_{R,E}$ are respectively expressed as,

$$y_{R,I} = \sqrt{\alpha}(\boldsymbol{H}^H \boldsymbol{W}\boldsymbol{s} + \boldsymbol{H}^H \boldsymbol{z} + \boldsymbol{n}_R) + \boldsymbol{n}_I, \quad (6)$$

$$y_{R,E} = \sqrt{1-\alpha}(\boldsymbol{H}^H \boldsymbol{W}\boldsymbol{s} + \boldsymbol{H}^H \boldsymbol{z} + \boldsymbol{n}_R), \quad (7)$$

where, $\alpha \in (0,1)$ is PS factor, $\boldsymbol{n}_I \sim \mathcal{CN}(0, \sigma_I^2 \mathbf{I}_{N_R})$ is the noise introduced by decoding. The worst secrecy rate that the system achieve can be expressed as (8) [8,15],

$$Rs(\alpha, \boldsymbol{W}, \boldsymbol{Z}) = \left[C_R(\alpha, \boldsymbol{W}, \boldsymbol{Z}) - \max_{\forall k \in \Pi} C_k(\boldsymbol{W}, \boldsymbol{Z}) \right]^+, \quad (8)$$

where, $[x]^+ = \max\{0, x\}$.

$$C_R(\alpha, \boldsymbol{W}, \boldsymbol{Z}) = \log\left|\mathbf{I}_{N_R} + \boldsymbol{\Lambda}_R^{-1} \alpha \boldsymbol{H}^H \boldsymbol{W}\boldsymbol{W}^H \boldsymbol{H}\right|,$$
$$\boldsymbol{\Lambda}_R = \alpha(\boldsymbol{H}^H \boldsymbol{Z}\boldsymbol{H} + \sigma_R^2 \mathbf{I}_{N_R}) + \sigma_I^2 \mathbf{I}_{N_R} \succ \mathbf{0}, \quad (9)$$

$$C_k(\boldsymbol{W}, \boldsymbol{Z}) = \log\left|\mathbf{I}_{N_E} + \boldsymbol{\Lambda}_k^{-1} \boldsymbol{G}_k^H \boldsymbol{W}\boldsymbol{W}^H \boldsymbol{G}_k\right|,$$
$$\boldsymbol{\Lambda}_k = \boldsymbol{G}_k^H \boldsymbol{Z}\boldsymbol{G}_k + \sigma_k^2 \mathbf{I}_{N_E} \succ \mathbf{0}, \quad (10)$$

$\boldsymbol{\Lambda}_R$ and $\boldsymbol{\Lambda}_k$ represent the interference noise covariance matrixs of authorized device R and k-th EH device, respectively. Equation (8) essentially reflects the gap between the decoding capabilities of authorized devices and EH devices.

The radio frequency energy received by the authorized device R and the k-th EH device are (11) and (12),

$$E_R = \eta(1-\alpha)Tr(\boldsymbol{H}^H(\boldsymbol{W}\boldsymbol{W}^H + \boldsymbol{Z})\boldsymbol{H} + \sigma_R^2 \mathbf{I}_{N_R}) \quad (11)$$

$$E_{EH,k} = \eta Tr(\boldsymbol{G}_k^H(\boldsymbol{W}\boldsymbol{W}^H + \boldsymbol{Z})\boldsymbol{G}_k + \sigma_k^2 \mathbf{I}_{N_E}), \quad (12)$$

where, $\eta \in (0,1]$ is the energy conversion efficiency of the energy receiver. The reason for using the linear energy harvesting mechanism here is that EH receivers of IoT devices often work at low input power, and the nonlinear energy harvesting mechanism shows a piecewise linear characteristic when the input power is relatively low, which can be approximated as a linear model [16]. At the same time, the linear energy harvesting mechanism has good

Table 1 Equipment state comparison table

	device 1	device 2	device 3⋯device K	device K+1
slot time	t	t	t	t
state	authorization	EH	EH	EH
slot time	$(1+l)t$	$(1+l)t$	$(1+l)t$	$(1+l)t$
state	EH	authorization	EH	EH

traceability. Therefore, we use the linear energy harvesting mechanism to facilitate subsequent analysis.

The goal of this paper is to optimize the global secrecy energy efficiency, which is defined as the ratio of the worst secrecy rate to the total power of the transmitter,

$$\mathrm{GSEE}(\alpha,\boldsymbol{W},\boldsymbol{Z})=\frac{Rs(\alpha,\boldsymbol{W},\boldsymbol{Z})}{P_{\mathrm{Total}}(\boldsymbol{W},\boldsymbol{Z})}. \tag{13}$$

Therefore, the global secrecy energy efficiency maximization problem can be described as **P1**,

$$\mathbf{P1:}\max_{\alpha,\boldsymbol{W},\boldsymbol{Z}} GSEE(\alpha,\boldsymbol{W},\boldsymbol{Z}) \tag{14a}$$

$$s.t.\ E_R(\alpha,\boldsymbol{W},\boldsymbol{Z})\ge \bar{e}_R, \tag{14b}$$

$$E_{EH,k}(\boldsymbol{W},\boldsymbol{Z})\ge \bar{e}_k, \tag{14c}$$

$$P_{\mathrm{Total}}(\boldsymbol{W},\boldsymbol{Z})\le P_{\max}, \tag{14d}$$

$$\boldsymbol{Z}\succeq\mathbf{0}, 0<\alpha<1. \tag{14e}$$

where, constraints (14a) and (14b) represent the energy harvesting constraints of authorized device R and EH device k, respectively. $\bar{e}_R$ and $\bar{e}_k$ are the lower limits of energy harvesting. (14d) represents the CPU's transmission power constraint, $P_{\max}$ is the maximum transmission power threshold. And (14e) represents the semidefinite character of the artificial noise covariance matrix and the value range of the power splitting factor α.

3. Resource allocation optimization strategy

3.1 Problem transformation and characteristic analysis

P1 is a typical fractional programming problem. In this paper, the Dinkelbach algorithm is used to transform the objective function. The Dinkelbach method can find the global optimal solution to the polynomial fractional programming problem. Suppose the maximum value of GSEE is $q^{\dagger}$,

$$q^{\dagger}=\max_{(\alpha,\boldsymbol{W},\boldsymbol{Z})\in\mathcal{X}} Rs(\alpha,\boldsymbol{W},\boldsymbol{Z})/P_{\mathrm{Total}}(\boldsymbol{W},\boldsymbol{Z}), \tag{15}$$

where, $\mathcal{X}=\{(\alpha,\boldsymbol{W},\boldsymbol{Z})|(4\text{-}14b)(4\text{-}14c)(4\text{-}14d)(4\text{-}14e)\}$ is the feasible field of **P1**.

Theorem 1: The optimal solution $\{\alpha^{\dagger},\boldsymbol{W}^{\dagger},\boldsymbol{Z}^{\dagger}\}$ can maximize the GSEE if and only if $q^{\dagger}$ is the only zero solution of the auxiliary function $F(q)$,

$$F(q)\triangleq\max_{(\alpha,\boldsymbol{W},\boldsymbol{Z})\in\mathcal{X}} Rs(\alpha,\boldsymbol{W},\boldsymbol{Z})-qP_{\mathrm{Total}}(\boldsymbol{W},\boldsymbol{Z}), \tag{16}$$

where, $Rs(\alpha,\boldsymbol{W},\boldsymbol{Z})\ge 0$ and $P_{\mathrm{Total}}(\boldsymbol{W},\boldsymbol{Z})>0$.

Proof: Please refer to [16] for the proof. □

Theorem 1 gives the basic idea of solving the fractional programming problem, and the designed iterative optimization algorithm can make the original problem converge to the optimal value. The specific operations are as follows:

(1) *Inner loop*: Given $q\ge 0$, solve the optimization problem shown in (16), then return the optimal solution $\left(\alpha^{(n)},\boldsymbol{W}^{(n)},\boldsymbol{Z}^{(n)}\right)$, where *n* is the number of iterations;

(2) *Outer loop*: Iterate q through the Dinkelbach algorithm until the optimal value $q^{\dagger}$ is obtained, and then return the optimal solution $\left(\alpha^{\dagger},\boldsymbol{W}^{\dagger},\boldsymbol{Z}^{\dagger}\right)$.

Due to the product terms of the variable α and $\boldsymbol{W}\boldsymbol{W}^H$ exist in the constraint (14b) and $Rs(\alpha,\boldsymbol{W},\boldsymbol{Z})$, (16) is still a non-convex function. In order to realize the equivalent transformation of the problem **P1**, let $\boldsymbol{Q}=\boldsymbol{W}\boldsymbol{W}^H$, $(1/\alpha)=t$, then construct a new optimization problem **P2**.

$$\mathbf{P2:}\max_{\boldsymbol{Q},\boldsymbol{Z},t,\gamma_1,\gamma_2} \gamma_1-\gamma_2-q(\mu Tr(\boldsymbol{Q}+\boldsymbol{Z})+P_C) \tag{17a}$$

$$s.t.\ \gamma_R\ge\gamma_1, \tag{17b}$$

$$\gamma_k\le\gamma_2, \boldsymbol{G}_k\in\boldsymbol{\Omega}_k, k\in\Pi, \tag{17c}$$

$$\eta(1-1/t)Tr(\boldsymbol{H}^H(\boldsymbol{Q}+\boldsymbol{Z})\boldsymbol{H}+\sigma_R^2\mathbf{I}_{N_R})\ge\bar{e}_R, \tag{17d}$$

$$\eta Tr(\boldsymbol{G}_k^H(\boldsymbol{Q}+\boldsymbol{Z})\boldsymbol{G}_k+\sigma_k^2\mathbf{I}_{N_E})\ge\bar{e}_k, \boldsymbol{G}_k\in\boldsymbol{\Omega}_k, k\in\Pi, \tag{17e}$$

$$\mu Tr(\boldsymbol{Q}+\boldsymbol{Z})+P_C\le P_{\max}, \tag{17f}$$

$$\boldsymbol{Q}\succeq\mathbf{0}, \boldsymbol{Z}\succeq\mathbf{0}, t>1, \tag{17g}$$

where, γ_1 and γ_2 are slack variables,

$$\begin{aligned}\gamma_R&=\log\left|\boldsymbol{H}^H(\boldsymbol{Z}+\boldsymbol{Q})\boldsymbol{H}+\sigma_R^2\mathbf{I}_{N_R}+t\sigma_I^2\mathbf{I}_{N_R}\right|\\&-\log\left|\boldsymbol{H}^H\boldsymbol{Z}\boldsymbol{H}+\sigma_R^2\mathbf{I}_{N_R}+t\sigma_I^2\mathbf{I}_{N_R}\right|,\end{aligned} \tag{18}$$

$$\begin{aligned}\gamma_k&=\log\left|\boldsymbol{G}_k^H(\boldsymbol{Z}+\boldsymbol{Q})\boldsymbol{G}_k+\sigma_k^2\mathbf{I}_{N_E}\right|\\&-\log\left|\boldsymbol{G}_k^H\boldsymbol{Z}\boldsymbol{G}_k+\sigma_k^2\mathbf{I}_{N_E}\right|, \boldsymbol{G}_k\in\boldsymbol{\Omega}_k, k\in\Pi\end{aligned}. \tag{19}$$

The problem **P2** is equivalent to the optimization problem defined by (16) if and only if the optimal solution of the **P2** makes the two sides of inequalities (17b) and (17c) obtain equal. Otherwise, without violating the constraint, the objective function can be maximized by increasing γ_1 or decreasing γ_2.

Due to $t>1$, thus (17d) can be converted to (20),

$$\frac{t\bar{e}_R}{(t-1)}-Tr(\boldsymbol{H}^H(\boldsymbol{Q}+\boldsymbol{Z})\boldsymbol{H}+\sigma_R^2\mathbf{I}_{N_R})\le 0. \tag{20}$$

Finding the Hessian matrix of equation (20), we can get $\nabla^2_{(20)}\succeq\mathbf{0}$, so (21) prove that the constraint (17d) is a convex set.

$$\nabla^2_{(20)}=\begin{bmatrix}\mathbf{0}&\mathbf{0}&0\\\mathbf{0}&\mathbf{0}&0\\0&0&\dfrac{2}{(\mathrm{t}-1)^3}\end{bmatrix}\succeq\mathbf{0}. \tag{21}$$

The objective function of **P2** is a linear function, and (17d)~(17g) are all convex constraints. In the constraints (17b) and (17c), γ_R and γ_k are the difference between the two concave functions, so the problem **P2** is still a non-convex problem. In order to resolve the non-convex constraints (17b) and (17c) in **P2**, the first-order Taylor series expansion method is used to linearly approximate γ_R and γ_k at a given point $(\boldsymbol{Q}^*,\boldsymbol{Z}^*,t^*)$.

For the first-order Taylor series expansion of multivariate matrix function $f(\boldsymbol{X},\boldsymbol{Y})$ at a given point $(\boldsymbol{X}^*,\boldsymbol{Y}^*)$, it can be expressed as (22),

$$\begin{aligned} f(\boldsymbol{X},\boldsymbol{Y}) &= f(\boldsymbol{X}^*,\boldsymbol{Y}^*) \\ &+Tr\left\{\left(\partial f(\boldsymbol{X},\boldsymbol{Y})/\partial\Psi(\boldsymbol{X})\right)^T_{\boldsymbol{X}=\boldsymbol{X}^*}\Psi(\boldsymbol{X}-\boldsymbol{X}^*)\right\} \\ &+Tr\left\{\left(\partial f(\boldsymbol{X},\boldsymbol{Y})/\partial\Psi(\boldsymbol{Y})\right)^T_{\boldsymbol{Y}=\boldsymbol{Y}^*}\Psi(\boldsymbol{Y}-\boldsymbol{Y}^*)\right\}. \end{aligned} \tag{22}$$

where, $\Psi(\boldsymbol{X})$ and $\Psi(\boldsymbol{Y})$ represent the subterms of the function $f(\boldsymbol{X},\boldsymbol{Y})$ containing the variables $\boldsymbol{X}$ and $\boldsymbol{Y}$, respectively. Assuming $f_1(\boldsymbol{Z},t\mathbf{I}_{N_R})=\log\left|\boldsymbol{H}^H\boldsymbol{Z}\boldsymbol{H}+\sigma_R^2\mathbf{I}_{N_R}+t\sigma_I^2\mathbf{I}_{N_R}\right|$, $f_2(\boldsymbol{Z},\boldsymbol{Q})=\log\left|\boldsymbol{G}_k^H(\boldsymbol{Z}+\boldsymbol{Q})\boldsymbol{G}_k+\sigma_k^2\mathbf{I}_{N_E}\right|$, take the Taylor series of $f_1(\boldsymbol{Z},t\mathbf{I}_{N_R})$ and $f_2(\boldsymbol{Z},\boldsymbol{Q})$ according to the matrix differentiation Theorem $\partial\left(\log|\boldsymbol{X}|\right)=Tr\left(\boldsymbol{X}^{-1}\partial\boldsymbol{X}\right)$. Bring the series expansion result into (18) and (19), we can get the approximated $\bar{\gamma}_R$ and $\bar{\gamma}_k$ shown in (23) and (24),

$$\begin{aligned} \bar{\gamma}_R =& \log\left|\boldsymbol{H}^H(\boldsymbol{Z}+\boldsymbol{Q})\boldsymbol{H}+\sigma_R^2\mathbf{I}_{N_R}+t\sigma_I^2\mathbf{I}_{N_R}\right|-\log\left|\boldsymbol{A}^*\right| \\ &-\frac{1}{\ln 2}Tr(\boldsymbol{A}^{*-1}\boldsymbol{H}^H(\boldsymbol{Z}-\boldsymbol{Z}^*)\boldsymbol{H})-\frac{1}{\ln 2}Tr(\boldsymbol{A}^{*-1}(t-t^*)\sigma_I^2\mathbf{I}_{N_R}), \end{aligned} \tag{23}$$

$$\begin{aligned} \bar{\gamma}_k =& \log\left|\boldsymbol{B}^*\right|+\frac{1}{\ln 2}Tr(\boldsymbol{B}^{*-1}\boldsymbol{G}_k^H(\boldsymbol{Z}-\boldsymbol{Z}^*+\boldsymbol{Q}-\boldsymbol{Q}^*)\boldsymbol{G}_k) \\ &-\log\left|\boldsymbol{G}_k^H\boldsymbol{Z}\boldsymbol{G}_k+\sigma_k^2\mathbf{I}_{N_E}\right|, \end{aligned} \tag{24}$$

where, $\boldsymbol{A}^*=\boldsymbol{H}^H\boldsymbol{Z}^*\boldsymbol{H}+\sigma_R^2\mathbf{I}_{N_R}+t^*\sigma_I^2\mathbf{I}_{N_R}$, $\boldsymbol{B}^*=\widehat{\boldsymbol{G}}_k^H(\boldsymbol{Z}^*+\boldsymbol{Q}^*)\widehat{\boldsymbol{G}}_k+\sigma_k^2\mathbf{I}_{N_E}$.

At this time, the constraints (17b) and (17c) can be approximately transformed into (25) and (26),

$$\bar{\gamma}_R \ge \gamma_1, \tag{25}$$

$$\bar{\gamma}_k \le \gamma_2. \tag{26}$$

After the above steps, the problem **P2** can be transformed into **P3**,

$$\mathbf{P3:}\ \max_{\boldsymbol{Q},\boldsymbol{Z},t,\gamma_1,\gamma_2}\ \gamma_1-\gamma_2-q(\mu Tr(\boldsymbol{Q}+\boldsymbol{Z})+P_C) \tag{27a}$$

$$s.t.\ (17\text{d})-(17\text{g}),(25),(26). \tag{27b}$$

However, due to the characteristics of the first-order Taylor series, which leads to $\gamma_R \ge \bar{\gamma}_R$, $\gamma_k \ge \bar{\gamma}_k$. The equal sign can only be established when $(\boldsymbol{Z},\boldsymbol{Q},t)=(\boldsymbol{Z}^*,\boldsymbol{Q}^*,t^*)$. Therefore, an iterative algorithm is proposed in this paper to make the solution obtained at a given point $(\boldsymbol{Z}^*,\boldsymbol{Q}^*,t^*)$ infinitely close to the optimal solution $(\boldsymbol{Z}^\dagger,\boldsymbol{Q}^\dagger,t^\dagger)$ of **P2**.

3.2 The transformation of uncertainty channel model

All the constraints in (27b) of problem **P3** are convex constraints and the objective function is a linear function. Therefore, the problem **P3** is a convex problem. However, both (26) and (17e) contain the uncertainty term introduced by $\boldsymbol{G}_k$. By using the linear matrix inequality (LMI) and introducing a relaxation variable $\{\theta_k,\zeta_k\}$ $(\theta_k\ge 0,\zeta_k\ge 0)$, the equation is equivalently transformed to eliminate uncertainty in the channel coefficient matrix [18]. $\bar{\gamma}_k\le\gamma_2$ can be equivalently converted to

$$\log\left|\boldsymbol{G}_k^H\boldsymbol{Z}\boldsymbol{G}_k+\sigma_k^2\mathbf{I}_{N_E}\right|\ge\log\zeta_k \tag{28}$$

$$\log\left|\boldsymbol{B}^*\right|+\frac{1}{\ln 2}Tr(\boldsymbol{B}^{*-1}\boldsymbol{G}_k^H(\boldsymbol{Z}-\boldsymbol{Z}^*+\boldsymbol{Q}-\boldsymbol{Q}^*)\boldsymbol{G}_k)\le\theta_k \tag{29}$$

$$\theta_k-\log\zeta_k-\gamma_2\le 0. \tag{30}$$

But due to the left and right sides of the inequality (28) are concave functions, the inequality is a non-convex set. Therefore, we transform it into a processable form by introducing Theorem 2.

Theorem 2: when the matrix A is a n-by-n semipositive matrix, i.e., $\mathbf{A}\succeq\mathbf{0}$, then the inequality (31) always holds if and only if $\text{rank}(\mathbf{A})\le 1$.

$$\left|\mathbf{I}+\mathbf{A}\right|\ge 1+Tr(\mathbf{A}), \tag{31}$$

Proof: Denote A and B to be the n-by-n semi-positive matrix, i.e., $\mathbf{A}\succeq\mathbf{0}$, $\mathbf{B}\succeq\mathbf{0}$. When matrix A and B satisfy the equation $\mathbf{AB}=\mathbf{BA}$, the following relationship holds [19],

$$\prod_{i=1}^{n}(\lambda_i\downarrow+\gamma_i\downarrow)\le\left|\mathbf{B}+\mathbf{A}\right|\le\prod_{i=1}^{n}(\lambda_i\downarrow+\gamma_i\uparrow), \tag{32}$$

where, $\lambda_1,\lambda_2,\lambda_3\cdots\lambda_n$ and $\gamma_1,\gamma_2,\gamma_3,\cdots\gamma_n$ are eigenvalues of matrix $\mathbf{B}$ and $\mathbf{A}$, respectively. The arrow points indicate the order of eigenvalues.

Denote $\mathbf{B}$ to be a n-order unit matrix, i.e., $\mathbf{B}=\mathbf{I}$. Then, inequalities (32) can be equivalently transformed into equation (33),

$$\begin{aligned} &\prod_{i=1}^{n}(1+\gamma_i\downarrow)\le\left|\mathbf{I}+\mathbf{A}\right|\le\prod_{i=1}^{n}(1+\gamma_i\uparrow) \\ &\Leftrightarrow\left|\mathbf{I}+\mathbf{A}\right|=\prod_{i=1}^{n}(1+\gamma_i)=1+\sum_{i=1}^{r}\gamma_i+\sum_{i\ne k}^{r}\gamma_i\gamma_k \\ &+\prod_{i=1}^{r}\gamma_i\ge 1+\sum_{i=1}^{r}\gamma_i=1+Tr(\mathbf{A}). \end{aligned} \tag{33}$$

where r is the rank of matrix $\mathbf{A}$.

When $r=\text{rank}(\mathbf{A})=1$, $\left|\mathbf{I}+\mathbf{A}\right|=1+Tr(\mathbf{A})$ in (33) holds. When $r=\text{rank}(\mathbf{A})=0$, $\mathbf{A}=\mathbf{0}$ and $\left|\mathbf{I}+\mathbf{A}\right|=1+Tr(\mathbf{A})$ always hold. Thus, Theorem 2 is proved. □

According to the conclusion in Theorem 2, the inequality (28) can be transformed into the equation (34).

$$Tr(\boldsymbol{G}_k^H\boldsymbol{Z}\boldsymbol{G}_k)\ge\sigma_k^{2(1-N_E)}\zeta_k-\sigma_k^2. \tag{34}$$

From vector quantized uncertainty channel coefficient matrix $\boldsymbol{G}_k=\widehat{\boldsymbol{G}}_k+\Delta\boldsymbol{G}_k$ $(k\in\Pi)$, we get $\boldsymbol{g}_k=vec(\boldsymbol{G}_k)$, $\widehat{\boldsymbol{g}}_k=vec(\widehat{\boldsymbol{G}}_k)$, $\Delta\boldsymbol{g}_k=vec(\Delta\boldsymbol{G}_k)$. From $\|\Delta\boldsymbol{G}_k\|_F\le\delta_k$, it is easily to know that $\left\|\Delta\boldsymbol{g}_k\right\|_2\le\delta_k$. Then the inequality (34) can be transformed into the group of inequalities (35), according to equation relation $Tr(\boldsymbol{A}^H\boldsymbol{BCD})=vec^H(\boldsymbol{A})(\boldsymbol{D}^T\otimes\boldsymbol{B})vec(\boldsymbol{C})$.

To further solve (35), the relevant theoretical basis is given by Theorem 3.

Theorem 3: (S- procedure) Define function:

$$h_j(\boldsymbol{x})=\boldsymbol{x}^H\boldsymbol{A}_j\boldsymbol{x}+2\text{Re}\{\boldsymbol{b}_j^H\boldsymbol{x}\}+c_j, \tag{36}$$

where, $\boldsymbol{A}_j$ is an *n*-order symmetric complex matrix, $\boldsymbol{A}_j\in\mathbb{C}^{n\times n}$. $\boldsymbol{b}_j$ is a complex vector, $\boldsymbol{b}_j\in\mathbb{C}^{n\times 1}$, and c_j is a real number, i.e. $c_j\in\mathbb{R}$. If $\hat{\boldsymbol{x}}$ satisfies $\hat{\boldsymbol{x}}^H\boldsymbol{A}_1\hat{\boldsymbol{x}}+2\text{Re}\{\boldsymbol{b}_1^H\hat{\boldsymbol{x}}\}+c_1<0$, a sufficient condition for relationship $h_1(\boldsymbol{x})\le 0\Rightarrow h_2(\boldsymbol{x})\le 0$ to be established is the existence of $\varsigma\ge 0$ makes $\varsigma\begin{bmatrix}\boldsymbol{A}_1 & \boldsymbol{b}_1\\ \boldsymbol{b}_1^H & c_1\end{bmatrix}-\begin{bmatrix}\boldsymbol{A}_2 & \boldsymbol{b}_2\\ \boldsymbol{b}_2^H & c_2\end{bmatrix}\succeq\mathbf{0}$ valid.

Proof: Please refer to [20] for the proof. □

According to Theorem 3, the group of inequalities (35) can be equivalently converted into linear matrix inequalities (37),

$$\begin{bmatrix}\varsigma_k\boldsymbol{I}+(\boldsymbol{I}\otimes\boldsymbol{Z}) & (\boldsymbol{I}\otimes\boldsymbol{Z})^H\widehat{\boldsymbol{g}}_k\\ \widehat{\boldsymbol{g}}_k^H(\boldsymbol{I}\otimes\boldsymbol{Z}) & \boldsymbol{F}_{1k}\end{bmatrix}\succeq\mathbf{0}, \tag{37}$$

where, $\boldsymbol{F}_{1k}=\widehat{\boldsymbol{g}}_k^H(\boldsymbol{I}\otimes\boldsymbol{Z})\widehat{\boldsymbol{g}}_k-\sigma_k^{2(1-N_E)}\zeta_k+\sigma_k^2-\varsigma_k\delta_k^2$, $\varsigma_k\ge 0$ is the auxiliary variable. Similarly, according to $Tr(\boldsymbol{A}^H\boldsymbol{BCD})=vec^H(\boldsymbol{A})(\boldsymbol{D}^T\otimes\boldsymbol{B})vec(\boldsymbol{C})$ and Theorem 3, inequality (29) can be converted to inequality (38),

$$\begin{cases}\Delta \boldsymbol{g}_k^H \Delta \boldsymbol{g}_k - \delta_k^2 \le 0, \\ -\widehat{\boldsymbol{g}}_k^H (\boldsymbol{I} \otimes \boldsymbol{Z}) \widehat{\boldsymbol{g}}_k - 2\mathrm{Re}\{\widehat{\boldsymbol{g}}_k^H (\boldsymbol{I} \otimes \boldsymbol{Z}) \Delta \boldsymbol{g}_k\} - \Delta \boldsymbol{g}_k^H (\boldsymbol{I} \otimes \boldsymbol{Z}) \Delta \boldsymbol{g}_k + \sigma_k^{2(1-N_E)} \zeta_k - \sigma_k^2 \le 0.\end{cases} \tag{35}$$

$$\begin{bmatrix} \upsilon_k \boldsymbol{I} - \boldsymbol{\Psi}_k & -\boldsymbol{\Psi}_k^H \widehat{\boldsymbol{g}}_k \\ -\widehat{\boldsymbol{g}}_k^H \boldsymbol{\Psi}_k & \boldsymbol{F}_{2k} \end{bmatrix} \succeq \boldsymbol{0}, \tag{38}$$

Where, $\boldsymbol{\Psi}_k = (\boldsymbol{B}^{*-1})^T \otimes (\boldsymbol{Z} - \boldsymbol{Z}^* + \boldsymbol{Q} - \boldsymbol{Q}^*)$, $\boldsymbol{F}_{2k} = -\upsilon_k \delta_k^2 - \ln\left|\boldsymbol{B}^*\right| + \theta_k \ln 2 - \widehat{\boldsymbol{g}}_k^H \boldsymbol{\Psi}_k \widehat{\boldsymbol{g}}_k$, $\upsilon_k \ge 0$ is the auxiliary variable.

Using the same treatment method as (29), (17e) can be equivalently converted into (39),

$$\begin{bmatrix} \lambda_k \boldsymbol{I} + (\boldsymbol{I} \otimes (\boldsymbol{Q} + \boldsymbol{Z})) & (\boldsymbol{I} \otimes (\boldsymbol{Q} + \boldsymbol{Z}))^H \widehat{\boldsymbol{g}}_k \\ \widehat{\boldsymbol{g}}_k^H (\boldsymbol{I} \otimes (\boldsymbol{Q} + \boldsymbol{Z})) & \Sigma \end{bmatrix} \succeq \boldsymbol{0}, \tag{39}$$

where, $\Sigma = -\lambda_k \delta_k^2 - \dfrac{\overline{e}_k}{\eta} + N_E \sigma_k^2 + \widehat{\boldsymbol{g}}_k^H (\boldsymbol{I} \otimes (\boldsymbol{Q} + \boldsymbol{Z})) \widehat{\boldsymbol{g}}_k$, $\lambda_k \ge 0$ is the auxiliary variable.

After the above processing, at a given point $(\boldsymbol{Q}^*, \boldsymbol{Z}^*, t^*)$, the problem **P3** is equivalently converted to the problem **P4**,

$$\textbf{P4:} \max_{\boldsymbol{Q},\boldsymbol{Z},t,\gamma_1,\gamma_2,\theta_k,\zeta_k,\varsigma_k,\upsilon_k,\lambda_k} \gamma_1 - \gamma_2 - q(\mu Tr(\boldsymbol{Q} + \boldsymbol{Z}) + P_C) \tag{40a}$$

$$s.t. (17\mathrm{d})(17\mathrm{f})(17\mathrm{g})(25)(30)(37)(38)(39), \tag{40b}$$

$$\varsigma_k \ge 0, \upsilon_k \ge 0, \lambda_k \ge 0, \theta_k \ge 0, \zeta_k \ge 0. \tag{40c}$$

Problem **P4** is the joint convex optimization problem about variable $\{\boldsymbol{Q}, \boldsymbol{Z}, t, \gamma_1, \gamma_2, \theta_k, \zeta_k, \varsigma_k, \upsilon_k, \lambda_k\}$, which can be solved by interior point method or Newton method. When the optimal solution $\{\boldsymbol{Q}^\dagger, \boldsymbol{Z}^\dagger, t^\dagger\}$ of the **P4** problem is obtained, one can use eigen-decomposition of $\boldsymbol{Q}^\dagger$ to get the corresponding $\boldsymbol{W}^\dagger$. Find the reciprocal of $t^\dagger$ to get the optimal value d of $\alpha^\dagger$.

Algorithm 1: Two-level iterative algorithm based on Dinkelbach

1. **Initialize** $q_i = 0$, $i = 0$, ε_1;
2. **Initialize** $\boldsymbol{Q}^{*(0)}$, $\boldsymbol{Z}^{*(0)}$, $t^{*(0)}$, ε_2;
3. **Repeat**
4. **Repeat**
5. Calculate problem **P4** using interior point method at $\{\boldsymbol{Q}^{*(n)}, \boldsymbol{Z}^{*(n)}, t^{*(n)}\}$, and assign the result to $\{\boldsymbol{Q}^{*(n+1)}, \boldsymbol{Z}^{*(n+1)}, t^{*(n+1)}\}$;
6. $n := n+1$;
7. **Until** $\left|f(q_i, \Xi^{(n)})\right| \le \varepsilon_1$
8. **If** $\left|f(q_i, \Xi^{(n)}) - f(q_i, \Xi^{(n-1)})\right| \le \varepsilon_2$
9. Convergence = true;
10. Return $q^\dagger = q_i + f(q_i, \Xi^{(n)}) / P_{\mathrm{Total}}(\Xi^{(n)})$ and $\Xi^\dagger = \Xi^{(n)}$
11. **Else** $q_{i+1} = q_i + f(q_i, \Xi^{(n)}) / P_{\mathrm{Total}}(\Xi^{(n)})$
9. Convergence = false;
10. **End**
11. $i := i+1$;
12. **Until** Convergence = true

($f(q_i, \Xi^{(n)})$ *is the objective function value of the n-th iteration of* ***P4**, Ξ is P4 feasible set*)

4. Convergence and algorithm complexity analysis

Under the given conditions q_i, **P4** is a convex problem, and the (n+1)-th iteration value in the inner loop is guaranteed to be the optimal value of the n-th iteration. Therefore, $f(q_i, \Xi^{(n)})$ is proved to be monotonically undiminished in the two-layer iterative optimization algorithm. At the same time, the constraint conditions stipulate the lower limit of energy harvesting and the upper limit of transmitted power, so $f(q_i, \Xi^{(n)})$ is guaranteed to converge to a certain value. Dinkelbach algorithm is applied to outer loop, which has its own convergence characteristics. Thus it can show that the algorithm proposed in this paper is convergent.

The computational complexity of algorithm 1 depends on the matrix dimension and the number of constraints of **P4**, which is an SDP problem. The time complexity of the iterative process is $\mathcal{O}(\sqrt{n}\log(1/\ell))$ [21], where ℓ denotes the solution accuracy and n denotes the dimension of matrix variables. In each iteration, the complexity of SDP problem solved by interior point method is $\mathcal{O}(mn^3 + m^2n^2 + m^3)$, where m is the number of constraints. Therefore, for each SDP optimization problem with fixed precision, the computational complexity of iterative solution using the interior point method is expressed as $\mathcal{O}((mn^{3.5} + m^2n^{2.5} + m^3n^{0.5}) \cdot \log(1/\ell))$. Combined with **P4**, the computational complexity of algorithm 1 is:

$\mathcal{O}((13(N_T + N_R + KN_E)^{3.5} + 13^2(N_T + N_R + KN_E)^{2.5} + 13^3(N_T + N_R + KN_E)^{0.5})\mathcal{L}_1\mathcal{L}_2\log(1/\ell))$

where, $\mathcal{L}_1$, $\mathcal{L}_2$ respectively represent the number of iterations of internal and external cycles.

5. Simulation results

In this section, we will prove the convergence and efficiency of the algorithm by numerical experiments. In the experiment, the number of antennas of CPU $N_T = 5$, authorized devices $N_R = 2$, potential eavesdropping devices $N_E = 2$ and eavesdropping devices are set $K = 2$. The circuit energy consumption of the downlink SWIPT MIMO network $P_C = 1\mathrm{W}$, the lower limit of energy harvesting $\overline{e}_1 = \overline{e}_2 = \overline{e}_k = 23\mathrm{dbm}$, the efficiency coefficient of the power amplifier μ and the energy conversion efficiency of the energy receiver η are all set as 1[22]. Channel coefficient matrix $\boldsymbol{H}$ from CPU to authorized device and potential eavesdropping device $\widehat{\boldsymbol{G}}_k$ are Gaussian random variables subject to $\mathcal{CN}(0, 10^{-2})$ [23]. In order to demonstrate the effectiveness of the proposed algorithm, four baseline algorithms are proposed. The four algorithms are the deterministic channel state information algorithm, the artificial noise free auxiliary algorithm, the fixed PS factor α=0.2 algorithm and the fixed PS factor α=0.5 algorithm. If there is no special instruction, the simulation results of each baseline algorithm are the average of 500 independent experiments used.

Fig. 2 shows the convergence of the proposed algorithm. In this experiment, the maximum transmission power of CPU is set as $P_{\max} = 2.5\mathrm{W}$, the lower limit of energy harvesting of authorized equipment is set as $\overline{e}_R = 22\mathrm{dBm}$, and the radius of channel uncertainty region is set as $\delta_1 = \delta_2 = 0.05$. The Fig. 2 proves that the two-level iterative optimization algorithm can converge after up to 2 iterations in the randomly generated four channels.

Fig. 3 shows the impact of the maximum transmission power of the CPU on the global secrecy energy efficiency for different reference algorithms. In the experiment, the lower limit of energy harvesting of authorized device is $\overline{e}_R = 22\mathrm{dBm}$, and the radius of channel uncertainty region is $\delta_1 = \delta_2 = 0.05$. Fig. 3 shows that with the increase of the maximum transmission power, the

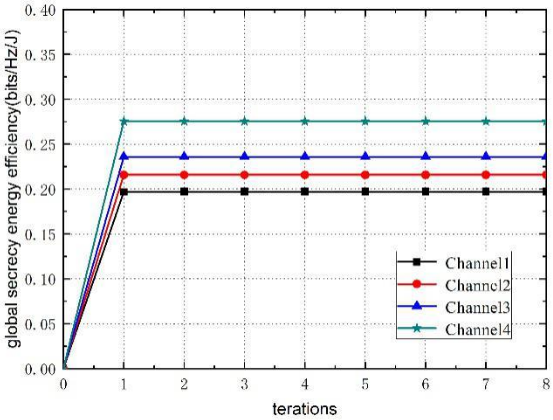

Fig. 2. The convergence of the proposed algorithm when four different channels are applied

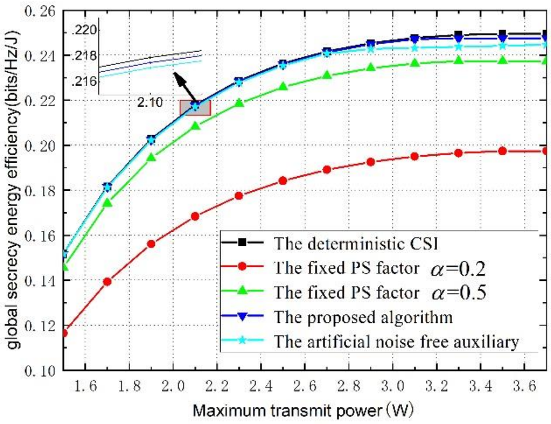

Fig. 3. The effects of the maximum transmission power on GSEE in different baseline algorithms

performance of GSEE under the deterministic channel state information mechanism is always the best. If the CPU can fully grasp the CSI between the eavesdropping devices, which can restrain the information eavesdropping to the maximum extent, so as to effectively improve the energy efficiency of global secrecy. But in the actual network scenario, it is difficult for the CPU to predict the CSI between the CPU and the eavesdropping device. In this paper, GSEE is maximized under the condition of uncertain CSI, which can ensure that the global energy efficiency of secrecy is close to the perfect channel state. In addition, Fig. 3 shows that the maximum global secrecy energy efficiency obtained by the algorithm is always higher than that of the artificial noise free auxiliary algorithm. Moreover, Fig. 3 shows that the GSEE obtained by the fixed PS algorithm is minimal. Compared with other mechanisms, the value of GSEE is the smallest. Because the fixed PS factor method only optimizes the precoding matrix, the artificial auxiliary noise covariance matrix would lack the flexibility of dynamic resource allocation.

Fig. 4 analyzes the impact of the maximum transmission power of CPU on the global secrecy energy efficiency when the radius of channel uncertainty region are 0.05, 0.07 and 0.09. As can be seen from Fig. 4, with the increase of maximum transmission power, GSEE shows an increasing trend, which is consistent with the curve trend in Fig. 3. It is worth noting that when the transmission power is higher than 3W, the global secrecy energy efficiency tends to be stable under the three uncertainty region radius. When the transmission power is lower than 2.8W, the values of GSEE

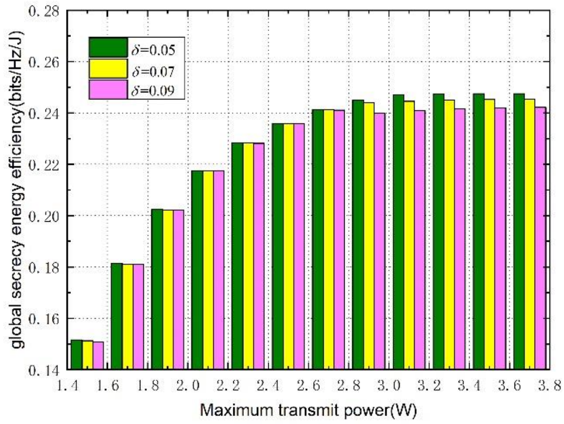

Fig. 4. The effects of the maximum transmission power on GSEE by varying the radius of uncertain region of different channels

obtained by the three uncertainty region radius are close to each other. When the transmission power is higher than 2.8W, the global secrecy energy efficiency decreases with the increase of the channel uncertainty region radius. This is because with the increase of the radius of the uncertainty region, the CPU will consume more energy to suppress the eavesdropping. Therefore, under the same transmission power, the larger the radius of the channel uncertainty region is, the smaller the global secrecy energy efficiency.

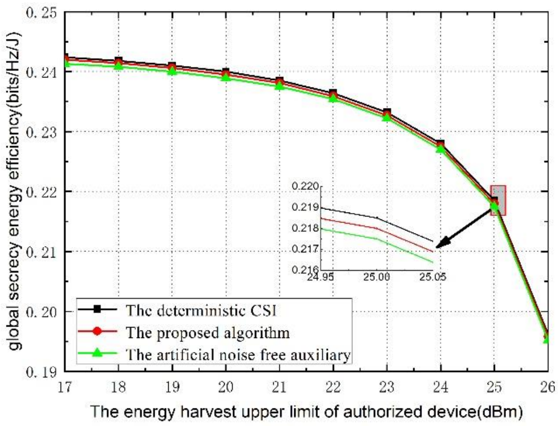

Fig. 5. The effects of the lower limit of harvested energy at the authorized equipment on GSEE in different baseline algorithms

Fig. 5 shows the effect of the lower limit of energy harvesting on the global secrecy energy efficiency of the three baseline algorithms. In this experiment, the maximum transmission power of CPU is set to $P_{\max}$ =2.7W, and the channel uncertainty region radius is set to $\delta_1 = \delta_2 = 0.05$. As shown in Figure 4-5, with the increase of the lower limit of energy collection for authorized equipment, the deterministic channel state information algorithm has the highest global secrecy energy efficiency, and the GSEE of the artificial noise free auxiliary algorithm is the lowest. The algorithm proposed in this paper is between the two algorithms. The increase of the lower limit of authorized device energy harvest makes the recovered RF power mainly used for the EH function. Because the total power is unchanged, the power used to avoid information leakage is correspondingly reduced, so the GSEE is reduced.

6. Conclusion

In this paper, the information security transmission mechanism is introduced into the objective function to make it more intuitively reflect the network security performance and resource utilization. Because of the non-convexity of the original optimization problem, the fractional programming problem is first transformed into subtraction equivalent form, and then some non-convex constraints are transformed by the first order Taylor technique expansion method. According to the transformed problem structure, a two-level iterative optimization algorithm is designed. Then, for the constraint conditions containing the radius of the uncertainty region of the eavesdropping channel, this paper uses the linear matrix inequality theory and the S-procedure for its equivalent transformation. The simulation experiment finally proves the effectiveness and reliability of the proposed algorithm, which can achieve the best global secrecy energy efficiency compared with other baseline algorithms.

Acknowledgements

The authors would like to thank Prof. Liang Xue, at Hebei University of Engineering, Xinping Guan, IEEE Fellow, at Shanghai Jiao Tong University and Yanyan Shen at Shenzhen Institutes of Advanced Technology, Chinese Academy of Sciences. The authors would also like to acknowledge Jianhui Liu, Nana Li, Yunfeng Wang, Yu Qin, Yao Ma, Chenyang Xu, and Wanqiang Qin at Hebei University of Engineering, and Yanlong Wang at Beijing University of Posts and Telecommunications for their input into the completion of this paper.

References

[1] Huang Y, Liu M, Liu Y. Energy-efficient SWIPT in IoT distributed antenna systems[J]. IEEE Internet of Things Journal, 2018, 5(4): 2646-2656.

[2] Xue X, Meng G. Secrecy Information Transmission Optimization of MIMO System[C]// 2019 Cross Strait Quad-Regional Radio Science and Wireless Technology Conference (CSQRWC). IEEE, 2019: 1-3.

[3] Hyun O, Seong-Jin K, Tae-Hak K. Research on the Application of GIS-Based Measures in the Advancement of the Construction Project Information System[J]. International Journal of Advances in Mechanical and Civil Engineering (IJAMCE), 2017, 4(6) :9-14.

[4] Chen X, Ng D W K, Chen H H. Secrecy wireless information and power transfer: Challenges and opportunities[J]. IEEE Wireless Communications, 2016, 23(2): 54-61.

[5] Xiong K, Wang B, Liu K J R. Rate-energy region of SWIPT for MIMO broadcasting under nonlinear energy harvesting model[J]. IEEE Transactions on Wireless Communications, 2017, 16(8): 5147-5161.

[6] Hadjira G ,Malika N . Investment in Renewable Energies for Sustainable Development [J]. International Journal of Advances in Mechanical and Civil Engineering (IJAMCE) , 2018, 5(3): 67-73.

[7] Shu X . Synchronization of Building Automation and Advance Information Systems as an Acceleration Tool in Moving Smart Grid Forward[J]. International Journal of Advances in Mechanical and Civil Engineering (IJAMCE) , 2016, 3(6):1-6.

[8] Boshkovska E, Zlatanov N, Dai L, et al. Secure SWIPT networks based on a non-linear energy harvesting model[C]//2017 IEEE Wireless Communications and Networking Conference Workshops (WCNCW). IEEE, 2017: 1-6.

[9] Yu H, Guo S, Yang Y, et al. Secrecy energy efficiency optimization for downlink two-user OFDMA networks with SWIPT[J]. IEEE Systems Journal, 2017, 13(1): 324-335.

[10] Lu Y, Xiong K, Fan P, et al. Global energy efficiency in secure MISO SWIPT systems with non-linear power-splitting EH model[J]. IEEE Journal on Selected Areas in Communications, 2018, 37(1): 216-232.

[11] Gong S, Xing C, Fei Z, et al. Secure communications for SWIPT over MIMO interference channel[C]//2016 IEEE 27th Annual International Symposium on Personal, Indoor, and Mobile Radio Communications (PIMRC). IEEE, 2016: 1-5.

[12] Yang Y, Zhao R. Research on the Joint Transmitter Beamforming Design for MIMO System with SWIPT[C]//2018 10th International Conference on Communications, Circuits and Systems (ICCCAS). IEEE, 2018: 180-184.

[13] Zhang H, Huang Y, Li S, et al. Energy-efficient precoder design for MIMO wiretap channels[J]. IEEE Communications Letters, 2014, 18(9): 1559-1562.

[14] Wang S, Wang B. Robust secure transmit design in MIMO channels with simultaneous wireless information and power transfer[J]. IEEE Signal Processing Letters, 2015, 22(11): 2147-2151.

[15] Sun Y, Ng D W K, Zhu J, et al. Multi-objective optimization for robust power efficient and secure full-duplex wireless communication systems[J]. IEEE Transactions on Wireless Communications, 2016, 15(8): 5511-5526.

[16] Xue L, Wang J L, Li J, et al. Precoding Design for Energy Efficiency Maximization in MIMO Half-Duplex Wireless Sensor Networks with SWIPT[J]. Sensors, 2019, 19(22): 4923.

[17] Long H, Xiang W, Zhang Y, et al. Secrecy capacity enhancement with distributed precoding in multirelay wiretap systems[J]. IEEE Transactions on Information Forensics and Security, 2012, 8(1): 229-238.

[18] Niu H, Guo D, Huang Y, et al. Robust energy efficiency optimization for secure MIMO SWIPT systems with non-linear EH model[J]. IEEE Communications Letters, 2017, 21(12): 2610-2613.

[19] Rostampoor J, Razavizadeh S M, Lee I. Energy efficient precoding design for SWIPT in MIMO two-way relay networks[J]. IEEE Transactions on Vehicular Technology, 2017, 66(9): 7888-7896.

[20] Boyd S, Vandenberghe L. Convex optimization[M]. UK: Cambridge university press, 2004.

[21] Zhou X, Li Q. Energy efficiency for SWIPT in MIMO two-way amplify-and-forward relay networks[J]. IEEE Transactions on Vehicular Technology, 2018, 67(6): 4910-4924.

[22] Niu H, Zhang B, Guo D, et al. Secrecy rate maximization for MIMO wiretap channels with a cooperative jammer using alternating optimization[C]// 2017 First International Conference on Electronics Instrumentation & Information Systems (EIIS). IEEE, 2017: 1-4.

[23] Nasir A A, Tuan H D, Duong T Q, et al. Secure and energy-efficient beamforming for simultaneous information and energy transfer[J]. IEEE Transactions on Wireless Communications, 2017, 16(11): 7523-7537.

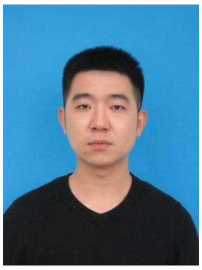

Jinlong Wang received his B.S. degree in electronic information engineering from Hebei University of Engineering, Handan, China, in 2017. He received the M.S. degree in electronic information engineering from Hebei University of Engineering in 2020. His research interests include wireless communications powered by energy harvesting, sensors network, MIMO communications, and resource allocation in SWIPT network. Email:jinlong_W1995@163.com

Na Li received the B.S. degree in computer science and technology from Tangshan University, Tangshan, China, in 2017. She received the M.S. degree in electronic information engineering from Hebei University of Engineering, Handan, China, in 2020. Her research interests include OFDM technology, convex optimization and resource allocation in simultaneous wireless

information and power transfer. Email: 424016301@qq.com

Datian Liu received his B.Eng degree in Electronic information engineering from Dalian Neusoft University of Information, Dalian, China, in 2018.
He is currently pursuing the M.S. degree in Computer Technology at Hebei University of Engineering. His research interest is Simultaneous Wireless Information and Power Transfer. Email:liudatian96@163.com

Lin Zuo received her B.Eng degree in IoT Engineering from Xuzhou Medical University, Xuzhou, China, in 2018. She is currently pursuing the M.S. degree in Computer Technology at Hebei University of Engineering. Her research interest is Simultaneous Wireless Information and Power Transfer.
Email:Lynne_Zuo@163.com